3D simulation of restrained alkali-silica reaction (ASR) expansion for numerical assessment of existing concrete structures

Zhanchong Shi[1*], Kathrine Stemland[1], Guomin Ji[1], Max Hendriks[1,2], Terje Kanstad[1]

*[1]Norwegian University of Science and Technology, Norway, szc1992czs@163.com, corresponding author**

[2] Delft University of Technology, the Netherlands

Abstract

Alkali-silica reaction (ASR) can pose a serious threat to existing reinforced concrete (RC) structures. ASR manifests as expansion leading to both additional load effects in the structure and material deterioration, which for structural members can lead to cracking of concrete and yielding of the reinforcement. The free ASR expansion is influenced by restraints from both external loading and internal reinforcement, a phenomenon known as restrained ASR expansion, which is anisotropic. A reliable method that can simulate the effect of ASR on a structural scale as a function of time is needed. The starting point of this modelling approach is free ASR strains that for instance can be deduced from cyclic compressive tests on extracted cylinders from the structure under investigation, frequently denoted Stiffness-Damage Testing (SDT). Furthermore, using the ABAQUS FE platform, a user subroutine to simulate the restrained ASR expansion strain in ASR-affected RC members was developed. Based on this programming, 3D finite element analyses on prism specimens with external loading or internal reinforcement were conducted. The results were compared and validated against experimental measurements. This investigation is part of a large project, denoted as MESLA, where the major objective is to obtain a more reliable assessment of ASR-affected concrete structures by coordinating inspection, material testing, and structural strength analysis.

Keywords: *concrete, ASR, restrained expansion, finite element method, user subroutine*

1 Introduction

Alkali-silica reaction (ASR) is a material degradation mechanism causing premature deterioration of concrete structures worldwide. ASR damage will lead to concrete expansion, cracking, and degraded material properties. Expansion can also contribute to tension in the steel reinforcement under, even to yielding [1]. Moreover, if concrete is restrained by surrounding non-reactive concrete, applied stress or reinforcement, the ASR expansion is reduced in the direction of restraint, and the dominant cracks form parallel to this direction [2]. This is the so-called restrained ASR effect, i.e., the ASR expansion is stress-dependent. The less compressive stress induced in concrete, the more ASR expansion and the more severe ASR damage. Hence, accurate modelling of restrained ASR expansion provides a solid foundation for more reliable structural performance assessment for concrete structures exposed to ASR.

Several modelling methods for ASR expansion have been proposed ranging from the micro-scale to the structural scale. Puatatsananon et al. [3] proposed a chemical reaction model focusing on the ion diffusion-reaction mechanisms. Esposito et al. [4] developed a meso-scale model by considering gel swelling simulation in both concrete matrix and aggregates. However, these models are complex since many model parameters are needed. Therefore, an accurate and relatively simple ASR expansion model is a necessity for engineering applications. In this study, based on laboratory ASR expansion test results carried out in MESLA [5], a free ASR expansion function was formulated. Moreover, based on the ABAQUS platform, an approach to model the restrained ASR expansion was developed and validated through comparison with experimental measurements.

This research activity is part of the research project MESLA (*Management and Extension of Service Life of infra-structures affected by Alkalisilica reactions (ASR)*) [6-8], funded by the Norwegian Research Council. The project period is 2021-2026, the project owner is the Norwegian University of

Science and Technology (NTNU), while the project partners are the bridge owners: the Norwegian Public Road Administration (NPRA), BaneNOR (railway bridge owner), Trøndelag County, and besides that Norconsult (consultant), SINTEF Community and SINTEF Narvik, and finally international partners, the universities Laval and Ottawa in Canada and Gustave Eiffel in France. The overall aim of MESLA is to build up new knowledge on how to manage and maintain existing ASR-affected structures in a technical, economical and environmental beneficial way, and verify how this knowledge can be applied to ensure structural safety and extend the service life of existing bridges in Norway.

2 Basic description of ASR expansion test

2.1 Expansion measurement

Free and restrained ASR expansion tests were conducted in 2019 and 2020, as shown in Table 1 and Fig.1 [5]. For free expansion, cube and prism samples with sizes of 230 × 230 × 230 mm and 230 × 230 × 300 mm were designed. The restrained expansion tests consisted of internally constrained samples, i.e., reinforced concrete (RC) prisms (labeled as RCPrism), and externally constrained samples which were labeled as LoadCube and were loaded by 3 MPa. In the LoadCube samples, Teflon plates were placed between the steel plates and the concrete cube to reduce friction. To ensure a consistent boundary condition, the free cube samples were made with a 10 mm-thick plate at the top and bottom surfaces. For the RCPrism, steel plates with a thickness of 10 or 15 mm were attached to the two end surfaces at the rebar direction (longitudinal direction). As shown in Fig.1, a Digital DEMEC Mechanical Strain Gauge instrument with 200 mm-gauge length was used to measure the ASR expansion. The measured expansion divided by the gauge length defined the expansion strains.

Table 1 Overview of designed samples [5].

Expansion types	Sample label	Rebar or external stress	Dimensions [mm]
Free expansion	2019-cube	—	230 × 230 × 230
	2019-prism	—	230 × 230 × 300
	2020-cube	—	230 × 230 × 230
	2020-prism	—	230 × 230 × 300
Restrained expansion: RC	2019-RCPrism-4d_s10	4d_s10 (ρ_s0.6%)	230 × 230 × 300
	2019-RCPrism-4d_s16	4d_s16 (ρ_s1.5%)	
	2020-RCPrism-4d_s16	4d_s16 (ρ_s1.5%)	
	2020-RCPrism-4d_s20	4d_s20 (ρ_s2.4%)	
Restrained expansion: external load	2019-LoadCube	3 MPa	230 × 230 × 230
	2020-LoadCube	3 MPa	

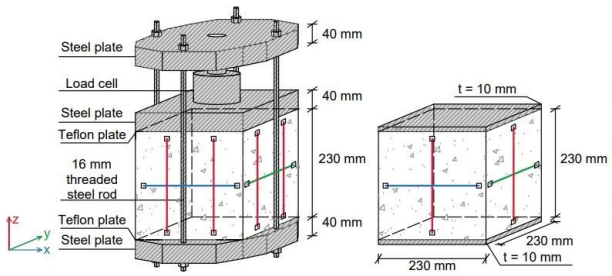

(a)

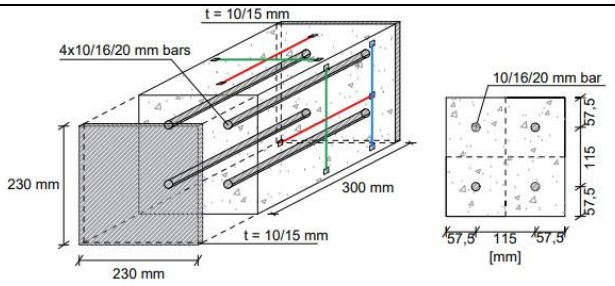

(b)

Fig. 1 Specimen and ASR expansion measurement design: (a) loaded cube and free cube; (b) RC prism[5].

2.2 Material properties

The concrete used has reactive aggregates, and is representative of concrete used in Norwegian infrastructure in the 1960s-1970s. The mix contains alkali-reactive coarse aggregate from crushed cataclasite (Ottersbo 4/16 mm), non-reactive sand mainly consisting of granite and gneiss (Årdal 0/4 mm), 457 kg/m^3 ordinary Portland cement (Norcem Industry, CEM I 42.5R with 1.24 % Na_2O_{eq}) [5]. This gives an alkali content of 5.6 kg Na_2O_{eq}/m^3.

Material properties of the concrete at 28-days, and steel rebars are listed in Table 2. In this table, f_{cm} and E_{cm} are the average cylinder compressive strength and elastic modulus of concrete, respectively; d_s, E_s, f_{sy}, and ε_{sy} are the diameter, elastic modulus, yielding strength, and yielding strain of the steel rebars, respectively.

2.3 Expansion results and free ASR expansion function

Fig.2 and Fig.3 show the measured free and restrained ASR expansion strain against time. The measured expansion displacements were divided by the gauge length to obtain the expansion strains. In these figures, for cube samples, cube-x/y/z denotes the direction of the measured expansion; for prism samples, prism-long is the expansion at the longitudinal (y) direction, prism-trans denotes the expansion at the transversal direction which is the average of the expansion in x and z directions.

Table 2 Material properties.

Concrete			Steel rebar			
Series	f_{cm} [MPa]	E_{cm} [MPa]	d_s [mm]	E_s [MPa]	f_{sy} [MPa]	ε_{sy} [‰]
2019	54.0	36487	10	207505	544.3	2.98
2020	43.2	34125	16	210559	536.2	3.11
-	-	-	20	218114	532.2	3.06

As shown in Fig. 2 and Fig. 3, all the expansion strains follow a similar trend comprising three distinct stages: the incubation stage, the cracking stage, and the stabilized stage. During the incubation stage, expansion progresses slowly until cracking occurs. Following this, the expansion proceeds at an approximately constant rate. Finally, the expansion rate decreases, and the final expansion stabilizes at an approximately constant value.

Based on all the free expansion data in Fig.2, a time-dependent free ASR expansion function was fitted as follows:

$$\varepsilon_{\mathrm{asr}}(t) = \varepsilon_{\mathrm{asr,end}} \left\{ 1 - \exp\left[-3.78 \cdot \left(\frac{t}{t_{\mathrm{end}}} \right)^{1.56} \right] \right\} \tag{1}$$

where: t_{end} is the measured final time, and $\varepsilon_{asr,end}$ is the measured free ASR expansion strain at time t_{end}.

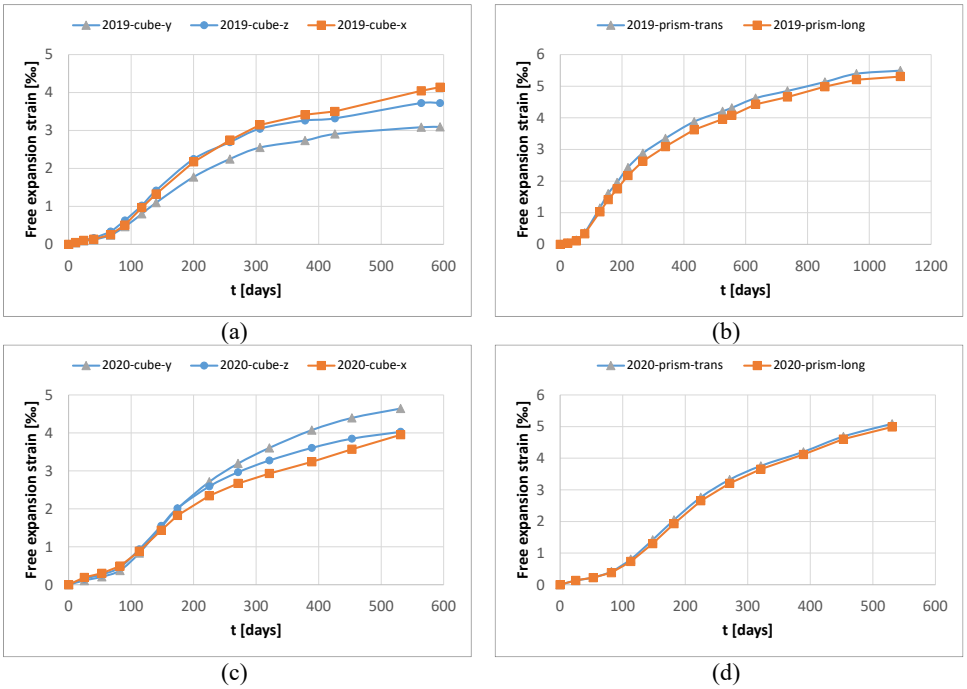

Fig. 2 Average free expansion history for cube and prism samples: (a) 2019 cubes; (b) 2019 prisms; (c) 2020 cubes; (d) 2020 prisms.

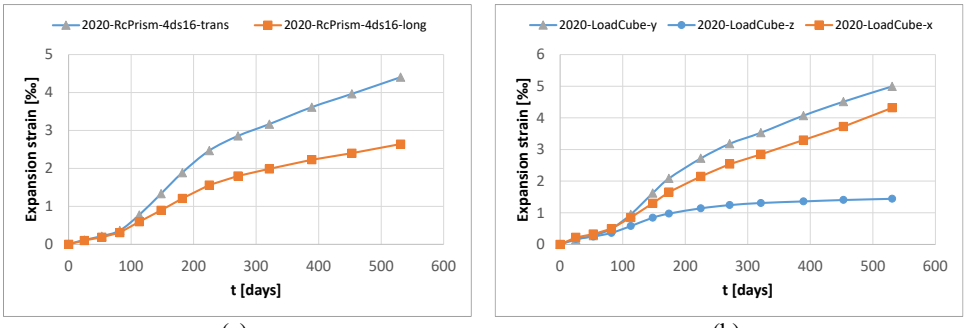

Fig. 3 Average expansion history for: (a) 2020-RcPrism-4d$_s$16; (b) 2020-LoadCube.

3 Finite element modelling and discussion

3.1 Modelling method

The ASR expansion is stress-dependent, and the developed ASR expansion or restrained ASR expansion can be expressed as:

$$\varepsilon_{\mathrm{asr,res}}(t) = w(\sigma) \cdot \varepsilon_{\mathrm{asr}}(t) \tag{2}$$

where: $\varepsilon_{\mathrm{asr,res}}(t)$ is the restrained ASR expansion strain; $\varepsilon_{\mathrm{asr}}(t)$ is the free ASR expansion strain, as shown in Eq.(1); $w(\sigma)$ is the stress-dependent function, as proposed by Charlwood et al. [9] and given as :

$$w(\sigma) = \begin{cases} 1 & \sigma \geq -\sigma_{\mathrm{L}} \\ 1 - \log\dfrac{(\sigma/-\sigma_{\mathrm{L}})}{(\sigma_{\mathrm{U}}/\sigma_{\mathrm{L}})} & -\sigma_{\mathrm{U}} \leq \sigma < -\sigma_{\mathrm{L}} \\ 0 & \sigma < -\sigma_{\mathrm{U}} \end{cases} \quad (3)$$

where the function parameters are given as: σ_U=6 MPa, σ_L=0.2 MPa.

In this study, the concrete normal stresses in the three coordinate axes of the global coordinate system, $\sigma_{c,x}$, $\sigma_{c,y}$, and $\sigma_{c,z}$, are adopted separately as the corresponding σ in Eq.(3). Therefore, the ASR expansion is anisotropic.

Considering that the expansion-induced compressive stresses of concrete in the tested sample were usually less than 5 MPa, the concrete creep strains were much less than the ASR-expansion strains, and therefore not considered.

The restrained ASR expansion was simulated based on the ABAQUS platform, which offers interfaces for secondary development through user subroutines [10]. The user subroutines USDFLD and UEXPAN, combined with utility routine GETVRM were used to apply the restrained ASR expansion strain. Moreover, the restrained ASR expansion was applied in the form of strain increment, as given in Eq.(4) according to Eq.(2):

$$\Delta\,\varepsilon_{\mathrm{asr,res}}(t) = w(\sigma) \cdot \Delta\,\varepsilon_{\mathrm{asr}}(t) \quad (4)$$

where: $\Delta\varepsilon_{asr,res}(t)$ is the restrained ASR expansion strain increment; and $\varepsilon_{asr}(t)$ is the free ASR expansion strain increment.

The simulation of restrained ASR expansion in each time step was achieved step by step as follows:

- Step 1: In USDFLD the stress tensor σ_{ij} of the previous increment was obtained through GETVRM giving $\sigma_{c,x}$, $\sigma_{c,y}$, and $\sigma_{c,z}$.
- Step 2: In USDFLD the three restrained ASR expansion strain increments $\Delta\varepsilon_{asr,res,x}$, $\Delta\varepsilon_{asr,res,y}$, $\Delta\varepsilon_{asr,res,z}$ were based on $\sigma_{c,x}$, $\sigma_{c,y}$, $\sigma_{c,z}$, and Eq.(4) and stored as state variables STATEVs.
- Step 3: In UEXPAN the restrained ASR strain increments were retrieved through the STATEVs and applied in the three respective coordinate axes.

3.2 Numerical validation and discussion

3.2.1 RC prism sample

The 2020-RcPrism-4ds16 sample and 2020-LoadCube were chosen to validate the ASR modelling method. The finite element (FE) model of 2020-RcPrism-4ds16 sample is shown in Fig.4(a). The concrete prism and steel plate were simulated by the linear interpolated 3D solid element C3D8R, and the steel rebars were modelled using the two-node truss element T3D2. The steel rebars were embedded in concrete. The connection between steel plate and concrete was simulated by ties. For the boundary condition, the vertical translational freedom *U*y of four corner points at the bottom surface was restrained. To simulate the restrained ASR expansion development, a total of 531 time steps were used, in which each step corresponds to 1 day.

The mesh size for the steel plate was 20 mm. For the concrete prism and steel rebars alternative mesh sizes of the 5 mm, 10 mm, and 20 mm were applied to investigate the effect on the simulation results. The target expansion displacement is the difference between the expansion displacements at the two measuring points (gauge length 200 mm) of the LVDTs. The obtained expansion displacement history is shown in Fig.5. In the figure, the rebar direction is the longitudinal direction, and the free direction is denoted transversal direction to investigate the restrained effect from steel rebars. As shown in the figure, the influence of mesh size on the expansions in rebar directions and free directions is relatively small.

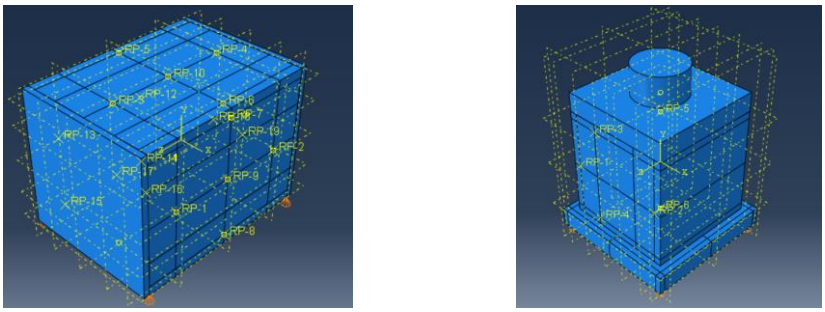

(a) (b)

Fig. 4 FE models for: (a) 2020-RcPrism-4ds16; (b) 2020-LoadCube.

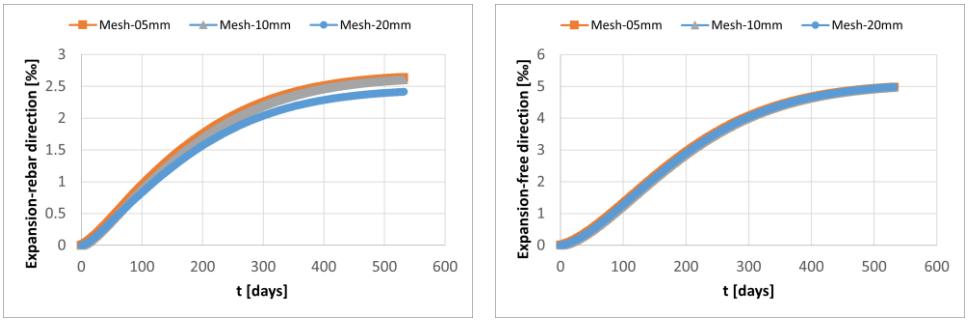

(a) (b)

Fig. 5 Expansion comparison from different mesh sizes for 2020-RcPrism-4d$_s$16: (a) rebar direction; (b) free direction.

The FEM results, with and without considering stress-dependent expansion (noted as FEM-SD and FEM-No SD, respectively) from the 10-mm mesh size were selected to be compared with experimental measurements, as illustrated in Fig.6. It is clear that the stress-dependence does not influence the expansion in the free direction significantly. While, when considering the stress-dependence, the FEM expansion correlates well with the experimental results. These results demonstrate the validity and feasibility of the proposed modelling method for restrained ASR expansion.

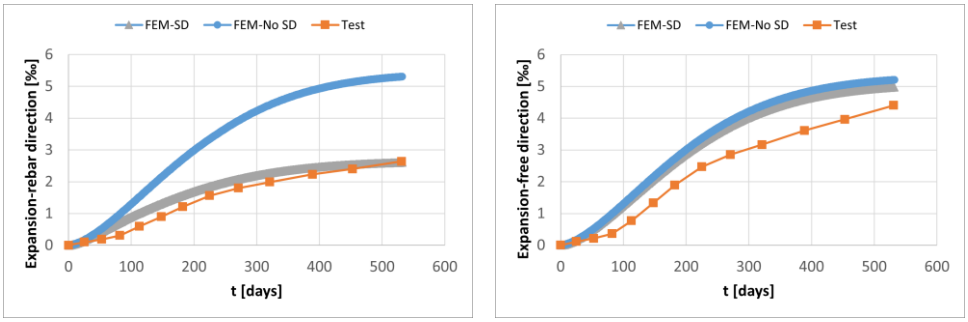

(a) (b)

Fig. 6 Expansion comparison between test and FEM results for 2020-RcPrism-4d$_s$16: (a) rebar direction; (b) free direction.

3.2.2 Loaded cube sample

The finite element (FE) model of the 2020-LoadCube sample is shown in Fig.4(b). The concrete cube, load cell, and steel plate were simulated by the solid element C3D8R. The load cell was tied to the upper steel plate, and the external force was applied to the top surface of the load cell. The assumed

properties of the steel-teflon-concrete interfaces will lead to different expansion results. Two methods were chosen and compared: fully tying the steel to the concrete and applying a contact connection. For the contact connection, the normal direction was modelled using a hard contact assumption while the tangential direction was simulated by a penalty method with three alternative coefficients of friction values of 0.6, 0.4, and 0.2. The boundary condition was again simulated by constraining the *U*x, *U*y, and *U*z displacements at the four bearing points on the lower steel plate. The loading consisted of applying the external load loading first in a single step, followed by 531 time steps with expansion.

The 20-mm mesh size was used for the steel plates and load cell. Alternative mesh sizes of the 5 mm, 10 mm and 20 mm for the concrete cube were compared to investigate their effect on the simulation results. The obtained expansion displacement history is shown in Fig.7. It is noted that the steel-teflon-concrete interface was simulated using tie in the FE models in Fig.7. Again, the influence of the mesh size on the expansions in load and free directions is relatively small.

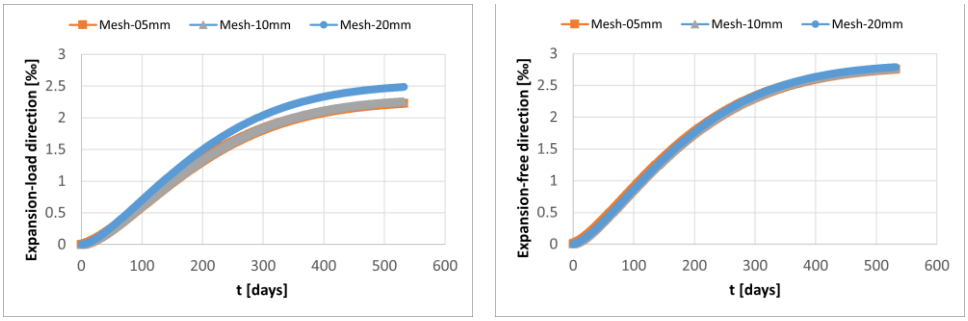

(a) (b)

Fig. 7 Expansion comparison from different mesh sizes for 2020-LoadCube: (a) load direction; (b) free direction.

Fig.8 shows the expansion comparison between the test and FE simulations with different steel-teflon-concrete interface modelling methods. Tie denotes the stiffest or the most rigid connection, while for the contact connection descending coefficients of friction from 0.6 to 0.2 indicate reduced tangential constraints. It is noted that all the FE simulations include stress-dependent ASR. As shown, the expansion in the free direction decreases with the increase of interface connection, while the expansion in the load direction presents an opposite trend. In general, the FE simulation with a coefficient of friction of 0.4 shows the best agreement with the test measurements.

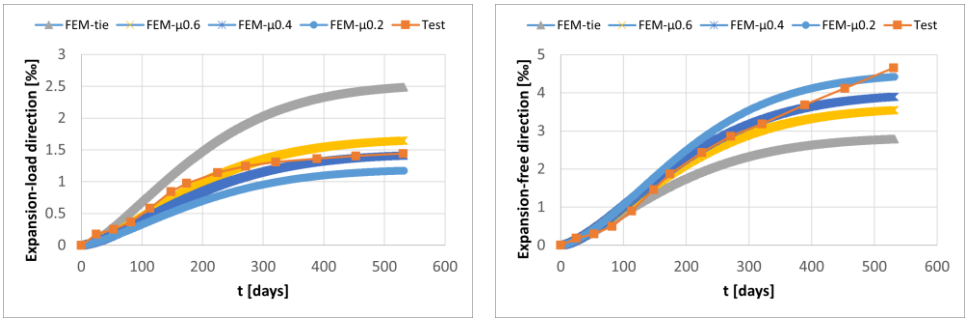

(a) (b)

Fig. 8 Steel-teflon-concrete interface modelling comparison for 2020-LoadCube: (a) load direction; (b) free direction.

4 Conclusion

Based on the test results and the numerical simulations, the main conclusions are:

1. The restrained effect of internal rebars or the external loading on the ASR expansion cannot be neglected, and must be considered to accurately simulate concrete structures suffering from ASR.

2. A finite element approach to model stress-dependent ASR expansion was developed based on ABAQUS user subroutines.
3. The feasibility of the developed stress-dependent ASR expansion modelling was validated by comparing the measurements and numerical simulations of externally loaded samples and rebar-reinforced samples. The FE model manages to simulate both the effect of constant stress and gradually developing stress by using the same stress dependence function with the same model parameters and applying incremental time steps.

Acknowledgements

This work was financially supported by the Research Council of Norway (326764).

References

[1] Godart, B., Sims, I., Nixon, P., Capra, B., de Rooij, M., Wood, J., ... & Avon, F. 2012. The RILEM guidance on appraisal and management of structures damaged by AAR. 14th International Conference on Alkali-Aggregate Reaction, 2012, Austin, USA.

[2] Institution of Structural Engineers. 1992. Structural effects of alkali-silica reaction: Technical guidance on the appraisal of existing structures. Institution of structural engineers.

[3] Puatatsananon, W., & Saouma, V. 2013. Chemo-mechanical micromodel for alkali-silica reaction. ACI Materials Journal, 110(1), 67.

[4] Esposito, R., & Hendriks, M. A. 2016. A multiscale micromechanical approach to model the deteriorating impact of alkali-silica reaction on concrete. Cement and Concrete Composites, 70, 139-152.

[5] Stemland, K. 2024. "Experimental and Structural Basis for Analysis and Assessment of Concrete Structures exposed to Alkali-Silica Reactions." PhD diss., Norwegian University of Science and Technology.

[6] Stemland, K., Rodum, E., & Kanstad, T. 2022. Stiffness damage testing of laboratory-cast alkali-silica reactive concrete and cores drilled from an existing concrete structure. In Proceedings of 16th ICAAR Conference, Lisbon, Portugal.

[7] Kanstad, T., Rodum, E., & Lindgård, J. 2024. Assessment of Norwegian Bridges Affected by ASR. In International Conference on Alkali-Aggregate Reaction in Concrete. Cham: Springer Nature Switzerland.

[8] Kanstad, T., Stemland, K., Rodum, E., & Lindgård, J. 2024. Assessment of Three Critically ASR-Deteriorated Bridges. In International Conference on Alkali-Aggregate Reaction in Concrete (pp. 419-427). Cham: Springer Nature Switzerland.

[9] Charlwood R, Solymar S, Curtis D. 1992. A review of alkali aggregate reactions in hydroelectric plants and dams. In: Proceedings of the international conference of alkali-aggregate reactions in hydroelectric plants and dams, vol. 129.

[10] Hibbitt. 2013. ABAQUS user subroutines reference manual (version 6.13). USA.